Efficient Compressed Sensing SENSE Parallel MRI Reconstruction with Joint Sparsity Promotion and Mutual Incoherence Enhancement*

Il Yong Chun[1], Ben Adcock[2], and Thomas M. Talavage[3]

***Abstract*— Magnetic resonance imaging (MRI) is considered a key modality for the future as it offers several advantages, including the use of non-ionizing radiation and having no known side effects on the human body, and has recently begun to serve as a key component of multi-modal neuroimaging. However, two major intrinsic problems exist: slow acquisition and intrusive acoustic noise. Parallel MRI (pMRI) techniques accelerate acquisition by reducing the duration and coverage of conventional gradient encoding. The under-sampled *k*-space data is detected with several receiver coils surrounding the object, using distinct spatial encoding information for each coil element to reconstruct the image. However, this scanning remains slow compared to typical clinical imaging (e.g. X-ray CT). Compressed Sensing (CS), a sampling theory based on random sub-sampling, has potential to further reduce the sampling used in pMRI, accelerating acquisition further. In this work, we propose a new CS SENSE pMRI reconstruction model promoting joint sparsity across channels and enhancing mutual incoherence to improve reconstruction accuracy from limited *k*-space data. For fast image reconstruction and fair comparisons, all reconstructions are computed with split-Bregman and variable splitting techniques. Numerical results show that, with the introduced methods, reconstruction performance can be crucially improved with limited amount of *k*-space data.**

I. INTRODUCTION

Compressed Sensing (CS) is an attractive theory for reconstruction of images from small numbers of measurements. Assuming a partial sensing matrix $\mathbf{P}_\Omega\mathbf{\Phi} \in \mathbb{C}^{N\times N}$ where $\mathbf{P}_\Omega$ is a diagonal projection matrix with m^{th} entry 1 if $m \in \Omega$ and 0 otherwise, $|\Omega| = M \ll N$ is chosen uniformly at random, $\mathbf{\Phi} \in \mathbb{C}^{N\times N}$ where $\{\phi_n\}_{n=1}^N$ is an orthonormal basis of $\mathbb{C}^N$, a sparsifying transform $\mathbf{\Psi} \in \mathbb{C}^{N\times N}$ where $\{\psi_n\}_{n=1}^N$ is an orthonormal basis of $\mathbb{C}^N$, and $\mathbf{y} = \mathbf{P}_\Omega\mathbf{y}^0 \in \mathbb{C}^N$ with $\mathbf{y}^0 = \mathbf{\Phi}\mathbf{x}$, the s-sparse solution in basis $\mathbf{\Psi}$ ($\|\mathbf{\Psi}\mathbf{x}\|_0 \triangleq |\text{supp}(\mathbf{\Psi}\mathbf{x})| \leq s \ll N$, where $\mathbf{x} \in \mathbb{C}^N$) of $\mathbf{y} = \mathbf{P}_\Omega\mathbf{\Phi}\mathbf{x}$ can be perfectly recovered with high probability by solving the following convex optimization problem:

$$\underset{\mathbf{x}}{\text{argmin}} \|\mathbf{\Psi}\mathbf{x}\|_1, \text{ s.t. } \mathbf{y} = \mathbf{P}_\Omega\mathbf{\Phi}\mathbf{x}$$

with sufficient number of measurements given by

$$M \geq \kappa\mu^2(\mathbf{U})Ns\log(N) \quad (1)$$

*This work is supported by the Indiana State Department of Health Spinal Cord and Brain Injury Research Fund.

[1]Il Yong Chun is with the School of Electrical and Computer Engineering, Purdue University, West Lafayette, IN 47907 USA (email: chuni@purdue.edu).

[2]Ben Adcock is with the Department of Mathematics, Purdue University, West Lafayette, IN 47907 USA (email: adcock@purdue.edu).

[3]Thomas M. Talavage is with the School of Electrical and Computer Engineering and Weldon School of Biomedical Engineering, Purdue University, West Lafayette, IN 47907 USA (email: tmt@purdue.edu).

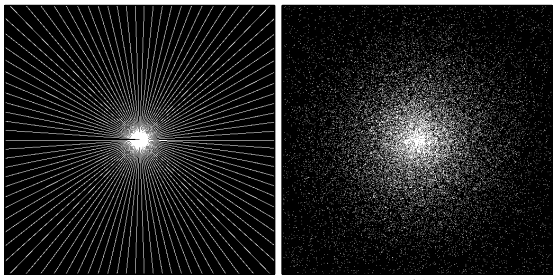

(a) (b)

Fig. 1. Sampling schemes (sampling ratio $\approx$ 10 %): (a) radial lines and (b) multi-level random sampling.

for some constant κ, where mutual coherence (MC) $\mu(\mathbf{U}) = \max_{m,n}|u_{m,n}| \in [1/\sqrt{N}, 1]$ and $\mathbf{U} = \mathbf{\Phi}\mathbf{\Psi}^{-1}$ [1], [2]. If, for example $\mathbf{\Phi}$ = DFT and $\mathbf{\Psi}$ = Identity so that $\mu(U) = 1/\sqrt{N}$, then (1) states that compressed sensing requires an optimally small number of measurements, up to a log factor. However, if $\mathbf{\Psi}$ = discrete Daubechies transform (DDT), then the MC is high, $\mu(\mathbf{U}) = 1$, and (1) predicts a barrier in the performance of CS. To overcome this, one must sample according to a nonuniform density, as recently explained in [3].

We consider the discrete pMRI model, in combination with SENSitivity Encoding (SENSE, [4]):

$$\mathbf{y} = \mathbf{F}_\mathbf{\Omega}\mathbf{S}\mathbf{x} + \mathbf{n},$$

where $\mathbf{y} = [\mathbf{y}_1^H \cdots \mathbf{y}_C^H]^H \in \mathbb{C}^{NC}$ is the noisy k-space observation in rectangular field of view (FOV), in which the k-space observation of the c^{th} coil is $\mathbf{y}_c = \mathbf{P}_\Omega\mathbf{y}_c^0 \in \mathbb{C}^N$ for $c = 1, \ldots, C$, C the number of coils; $\mathbf{F}_\mathbf{\Omega} = \mathbf{I}_C \otimes \mathbf{P}_\Omega\mathbf{\Phi} \in \mathbb{C}^{NC\times NC}$, where $\mathbf{P}_\Omega\mathbf{\Phi} \in \mathbb{C}^{N\times N}$ is a partial DFT matrix with a corresponding full DFT matrix $\mathbf{\Phi} \in \mathbb{C}^{N\times N}$; $\mathbf{S} = [\mathbf{S}_1^H \cdots \mathbf{S}_C^H]^H \in \mathbb{C}^{NC\times N}$, in which $\mathbf{S}_c = diag(\mathbf{s}_c) \in \mathbb{C}^{N\times N}$, where $\mathbf{s}_c$ is the sensitivity profile for c^{th} coil; $\mathbf{x} \in \mathbb{C}^N$ is the unknown image to be reconstructed; and noise $\mathbf{n} \in \mathbb{C}^{NC}$. Here $diag(\cdot)$ denotes the conversion of a vector into a diagonal matrix.

In this work, we propose a new CS SENSE pMRI reconstruction model promoting joint sparsity (JS, [5], [6], [7]) across the channels to improve reconstruction accuracy from limited amounts of k-space data. To overcome the aforementioned MC barrier, a multi-level sampling scheme ([3]) is applied. Such a scheme may not be realistic in practical 2D imaging, so we also provide results showing improved accuracy with radial line sampling. For fast image reconstruction and fair comparisons, all the models are solved with split-Bregman (SB, [8]) and variable splitting (VS, [9]) techniques. In this framework, the new model has an additional advantage of an efficient reconstruction using a

978-1-4244-7929-0/14/$26.00 ©2014 IEEE

combination of multiple sparsifying systems, e.g. DDT and total vatiation (TV).

II. METHODS

By separating the original problem into several subproblems which can be solved more simply, the split-Bregman (SB) technique is known to exhibit rapid and efficient convergence for l_1-norm minimization. The variable splitting (VS) technique has been applied on different occasions to solve problems more efficiently. An application of these techniques leads here to the fair comparison of all models.

A. Efficient conventional CS SENSE pMRI Reconstruction by SB using VS

The following is a conventional CS SENSE pMRI reconstruction model [10]:

$$\underset{\mathbf{x}}{\operatorname{argmin}} \|\mathbf{\Psi x}\|_1, \text{ s.t. } \|\mathbf{y}-\mathbf{F_\Omega S x}\|_2^2 < \eta. \tag{2}$$

By simplified Bregman iteration [11], (2) can be reduced to a sequence of unconstrained problems:

$$\mathbf{x}^{(k+1)} = \underset{\mathbf{x}^{(k)}}{\operatorname{argmin}} \|\mathbf{\Psi x}^{(k)}\|_1 + (\alpha/2)\|\mathbf{y}^{(k)} - \mathbf{F_\Omega S x}^{(k)}\|_2^2; \tag{3}$$

$$\mathbf{y}^{(k+1)} = \mathbf{y}^{(k)} + \mathbf{y} - \mathbf{F_\Omega S x}^{(k+1)}. \tag{4}$$

After transforming (3) to a constrained problem through VS (i.e. $\mathbf{d}_\mathbf{\Psi}^{(k)} = \mathbf{\Psi x}^{(k)}$ and $\mathbf{d}_\mathbf{S}^{(k)} = \mathbf{S x}^{(k)}$), (3) becomes equivalent to the following two-phase algorithm, according to SB:

$$\begin{aligned}
&(\mathbf{x}^{(k+1)}, \mathbf{d}_\mathbf{S}^{(k+1)}, \mathbf{d}_\mathbf{\Psi}^{(k+1)}) \\
&= \underset{\mathbf{x}^{(k)}, \mathbf{d}_\mathbf{S}^{(k)}, \mathbf{d}_\mathbf{\Psi}^{(k)}}{\operatorname{argmin}} \|\mathbf{d}_\mathbf{\Psi}^{(k)}\|_1 + (\alpha/2)\|\mathbf{y}^{(k)} - \mathbf{F_\Omega d}_\mathbf{S}^{(k)}\|_2^2 + \\
&\qquad (\nu/2)\|\mathbf{d}_\mathbf{S}^{(k)} - \mathbf{S x}^{(k)} - \mathbf{b}_\mathbf{S}^{(k)}\|_2^2 + \\
&\qquad (\beta/2)\|\mathbf{d}_\mathbf{\Psi}^{(k)} - \mathbf{\Psi x}^{(k)} - \mathbf{b}_\mathbf{\Psi}^{(k)}\|_2^2; \\
&\mathbf{b}_\mathbf{S}^{(k+1)} = \mathbf{b}_\mathbf{S}^{(k)} + \mathbf{S x}^{(k+1)} - \mathbf{d}_\mathbf{S}^{(k+1)} \\
&\mathbf{b}_\mathbf{\Psi}^{(k+1)} = \mathbf{b}_\mathbf{\Psi}^{(k)} + \mathbf{\Psi x}^{(k+1)} - \mathbf{d}_\mathbf{\Psi}^{(k+1)}.
\end{aligned} \tag{5}$$

Because the l_1 and l_2 components are decomposed, we can solve (5) efficiently by minimizing it separately with respect to $\mathbf{x}^{(k)}$, $\mathbf{d}_\mathbf{S}^{(k)}$, and $\mathbf{d}_\mathbf{\Psi}^{(k)}$. The $\mathbf{x}^{(k+1)}$ can be easily obtained:

$$\begin{aligned}
\mathbf{x}^{(k+1)} =& \big(\beta\mathbf{I} + \nu\mathbf{S}^H\mathbf{S}\big)^{-1} \\
&\big(\beta\mathbf{\Psi}^H(\mathbf{d}_\mathbf{\Psi}^{(k)} - \mathbf{b}_\mathbf{\Psi}^{(k)}) + \nu\mathbf{S}^H(\mathbf{d}_\mathbf{S}^{(k)} - \mathbf{b}_\mathbf{S}^{(k)})\big).
\end{aligned}$$

The $\mathbf{d}_\mathbf{\Psi}^{(k)}$ can be calculated quickly by an element-wise soft-shrinkage operator defined by $softshrink(x, \alpha) = (x/|x|)max(|x| - \alpha, 0)$:

$$d_{\mathbf{\Psi},n}^{(k+1)} = softshrink([\mathbf{\Psi x}^{(k+1)}]_n + b_{\mathbf{\Psi},n}^{(k)}, 1/\beta)$$

for $n = 1, \ldots, N$. Hence, the total reconstruction time depends predominantly on the cost to calculate $\mathbf{d}_\mathbf{S}^{(k+1)}$. Using only C pairs of *fft*$_2$ and *ifft*$_2$, $\mathbf{d}_\mathbf{S}^{(k+1)}$ can be obtained:

$$\mathbf{d}_\mathbf{S}^{(k+1)} = \mathbf{\Phi}_\mathbf{C}^H\mathbf{\Lambda}^{-1}\mathbf{\Phi_C z},$$

where diagonal matrix $\mathbf{\Lambda} = \alpha\mathbf{P}_\mathbf{\Omega}^T\mathbf{P_\Omega} + \nu\mathbf{I}$, $\mathbf{z} = \alpha\mathbf{F}_\mathbf{\Omega}^H\mathbf{y}^{(k)} + \nu(\mathbf{S x}^{(k+1)} + \mathbf{b}_\mathbf{S}^{(k)})$, $\mathbf{\Phi_C} = \mathbf{I}_C \otimes \mathbf{\Phi}$, and $\mathbf{P_\Omega} = \mathbf{I}_C \otimes \mathbf{P}_\Omega$.

B. Efficient CS SENSE pMRI Reconstruction Promoting JS by SB using VS

The conventional CS SENSE pMRI model (2) does not fully exploit the relationship between the images in each coil; in particular, their shared sparsity patterns. The proposed CS SENSE pMRI reconstruction model using joint sparsity (JS, $\|\cdot\|_{2,1}$) is given by:

$$\underset{\mathbf{x}}{\operatorname{argmin}} \|\mathbf{\Psi_C S x}\|_{2,1}, \text{ s.t. } \|\mathbf{y}-\mathbf{F_\Omega S x}\|_2^2 < \eta. \tag{6}$$

where $\mathbf{\Psi_C} = \mathbf{I}_C \otimes \mathbf{\Psi}$ and $\|\boldsymbol{\psi}\|_{2,1} = \sum_{n=1}^{N}\sqrt{\sum_{c=1}^{C}|\psi_{nc}|^2}$. $\|\cdot\|_{2,1}$ is a convex functional that exploits cross-channel dependencies between wavelet coefficients in the same spatial positions [5], [6], [7]. By simplified Bregman iteration, (6) can be reduced to a sequence of unconstrained problems:

$$\mathbf{x}^{(k+1)} = \underset{\mathbf{x}^{(k)}}{\operatorname{argmin}} \|\mathbf{\Psi_C S x}^{(k)}\|_{2,1} + (\alpha/2)\|\mathbf{y}^{(k)} - \mathbf{F_\Omega S x}^{(k)}\|_2^2; \tag{7}$$

$$\mathbf{y}^{(k+1)} = \mathbf{y}^{(k)} + \mathbf{y} - \mathbf{F_\Omega S x}^{(k+1)}. \tag{8}$$

After transforming (7) to a constrained problem through VS (i.e. $\mathbf{d}_\mathbf{S}^{(k)} = \mathbf{S x}^{(k)}$ and $\mathbf{d}_\mathbf{\Psi}^{(k)} = \mathbf{\Psi_C d}_\mathbf{S}^{(k)}$), (7) is equivalent to the following two phase algorithm, based on the SB method:

$$\begin{aligned}
&(\mathbf{x}^{(k+1)}, \mathbf{d}_\mathbf{S}^{(k+1)}, \mathbf{d}_\mathbf{\Psi}^{(k+1)}) \\
&= \underset{\mathbf{x}^{(k)}, \mathbf{d}_\mathbf{S}^{(k)}, \mathbf{d}_\mathbf{\Psi}^{(k)}}{\operatorname{argmin}} \|\mathbf{d}_\mathbf{\Psi}^{(k)}\|_{2,1} + (\alpha/2)\|\mathbf{y}^{(k)} - \mathbf{F_\Omega d}_\mathbf{S}^{(k)}\|_2^2 + \\
&\qquad (\nu/2)\|\mathbf{d}_\mathbf{S}^{(k)} - \mathbf{S x}^{(k)} - \mathbf{b}_\mathbf{S}^{(k)}\|_2^2 \\
&\qquad (\beta/2)\|\mathbf{d}_\mathbf{\Psi}^{(k)} - \mathbf{\Psi_C d}_\mathbf{S}^{(k)} - \mathbf{b}_\mathbf{\Psi}^{(k)}\|_2^2; \\
&\mathbf{b}_\mathbf{S}^{(k+1)} = \mathbf{b}_\mathbf{S}^{(k)} + \mathbf{S x}^{(k+1)} - \mathbf{d}_\mathbf{S}^{(k+1)} \\
&\mathbf{b}_\mathbf{\Psi}^{(k+1)} = \mathbf{b}_\mathbf{\Psi}^{(k)} + \mathbf{\Psi_C d}_\mathbf{S}^{(k+1)} - \mathbf{d}_\mathbf{\Psi}^{(k+1)}.
\end{aligned} \tag{9}$$

Because l_1 and l_2 components are decomposed, we can solve (9) efficiently by minimizing it separately with respect to $\mathbf{x}^{(k)}$, $\mathbf{d}_\mathbf{S}^{(k)}$, and $\mathbf{d}_\mathbf{\Psi}^{(k)}$. The $\mathbf{x}^{(k+1)}$ can be calculated easily:

$$\mathbf{x}^{(k+1)} = (\mathbf{S}^H\mathbf{S})^{-1}\mathbf{S}^H(\mathbf{d_S}^{(k)} - \mathbf{b_S}^{(k)}).$$

The $\mathbf{d}_\mathbf{\Psi}^{(k)}$ can be obtained quickly by an element-wise joint soft-shrinkage operator defined by $Jsoftshrink(\mathbf{x}, \gamma) = (\mathbf{x}/\|\mathbf{x}\|_2)\text{max}(\|\mathbf{x}\|_2 - \gamma, 0)$:

$$\mathbf{d}_{\mathbf{\Psi},n}^{(k+1)} = Jsoftshrink([\mathbf{\Psi_C d}_\mathbf{S}^{(k+1)}]_n + \mathbf{b}_{\mathbf{\Psi},n}^{(k)}, 1/\beta),$$

for $n = 1, \ldots, N$, where $[\mathbf{\Psi_C d}_\mathbf{S}^{(k+1)}]_n = [[\mathbf{\Psi_C d}_\mathbf{S}^{(k+1)}]_{n1}; \cdots; [\mathbf{\Psi_C d}_\mathbf{S}^{(k+1)}]_{nC}]$. Therefore, the total reconstruction time heavily depends on the computational cost to obtain $\mathbf{d}_\mathbf{S}^{(k+1)}$ from (9). The minimization of (9) with respect to $\mathbf{d}_\mathbf{S}^{(k)}$ can be solved analytically as follows:

$$\mathbf{d}_\mathbf{S}^{(k+1)} = \mathbf{\Phi}_\mathbf{C}^H\mathbf{\Lambda}^{-1}\mathbf{\Phi_C z},$$

where diagonal matrix $\mathbf{\Lambda} = \alpha\mathbf{P}_\mathbf{\Omega}^T\mathbf{P_\Omega} + (\beta + \nu)\mathbf{I}$, $\mathbf{z} = \alpha\mathbf{F}_\mathbf{\Omega}^H\mathbf{y}^{(k)} + \beta\mathbf{\Psi}_\mathbf{C}^H(\mathbf{d}_\mathbf{\Psi}^{(k)} - \mathbf{b}_\mathbf{\Psi}^{(k)}) + \nu(\mathbf{S x}^{(k+1)} + \mathbf{b}_\mathbf{S}^{(k)})$. As before, the main computation here is C pairs of *fft*$_2$ and *ifft*$_2$.

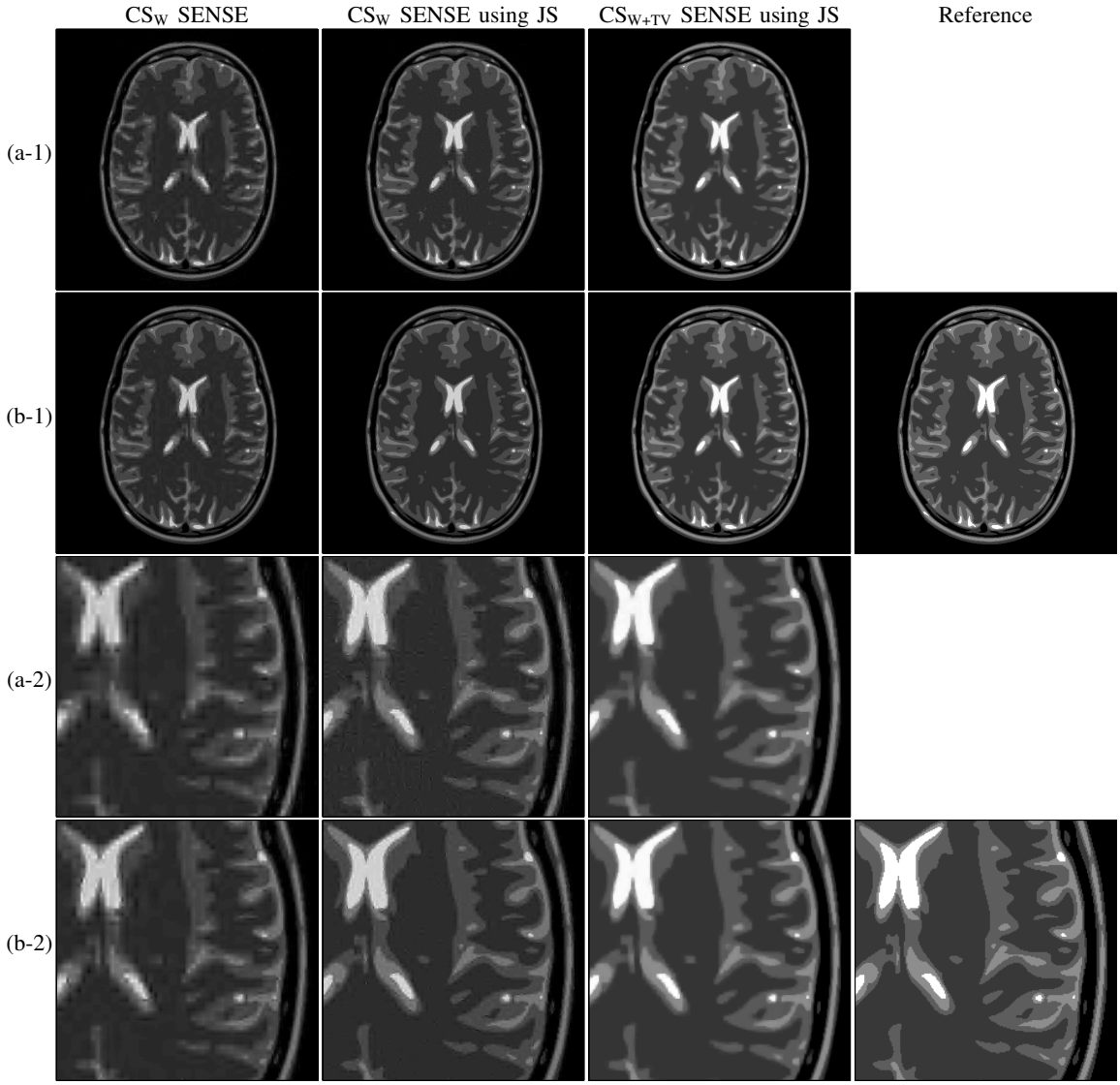

Fig. 2. Comparison of 512×512 reconstructed images from different CS SENSE pMRI reconstruction and sampling methods ($C = 4$, sampling percentage ≈ 10 %): (a-1) whole image based on radial lines, (b-1) whole image based on multi-level random sampling, (a-2) zoomed-in image based on radial lines, and (b-2) zoomed-in image based on multi-level random sampling.

Another benefit of this approach is an efficient incorporation of current model with TV minimization:

$$\begin{aligned} \underset{\mathbf{x}}{\operatorname{argmin}} \; & \|\mathbf{\Psi_C S x}\|_{2,1} + \|\mathbf{G}_{1,\mathbf{C}}\mathbf{S x}\|_{2,1} + \\ & \|\mathbf{G}_{2,\mathbf{C}}\mathbf{S x}\|_{2,1}, \text{ s.t. } \|\mathbf{y} - \mathbf{F_\Omega S x}\|_2^2 < \eta, \end{aligned} \tag{10}$$

where $\mathbf{G}_{1,\mathbf{C}} = \mathbf{I}_C \otimes \mathbf{G}_1$ with horizontal direction gradient transform $\mathbf{G}_1 \in \mathbb{C}^{N\times N}$, and $\mathbf{G}_{2,\mathbf{C}} = \mathbf{I}_C \otimes \mathbf{G}_2$ with vertical direction gradient transform $\mathbf{G}_2 \in \mathbb{C}^{N\times N}$. Noting that $\mathbf{G}_1^T\mathbf{G}_1 + \mathbf{G}_2^T\mathbf{G}_2$ has circulant structure under periodic boundary condition, (10) is solved in a similar way as above.

C. Multi-Level Random Sampling

Nonuniform density random sampling is necessary to overcome the MC barrier in CS [3]. So-called multi-level random sampling provides an optimized strategy to this end [3]. Assuming that normalized field-of-view (FOV) of k-space is in $[-1, 1]^2$, inside the FOV, there exist n regions delimited by $n-1$ equi-spaced concentric circles and the full square. Let the circles have radius $r_i = m$ if $i = 0$ and $r_i = i(1-m)/(n-1)$ if $i = 1, \ldots, n-1$, where $0 \le m < 1$. The uniform probability densities for each regions is defined:

$$p_i = \exp\big(-b \cdot (i/n)^a\big),$$

where $i = 0, \ldots, n$ and $a, b > 0$. Note that the sampling ratio decreases as $i \to n$. In Fig. 1, this scheme is graphically illustrated with radial line sampling.

III. SIMULATION RESULTS AND DISCUSSIONS

The introduced CS pMRI reconstruction models are named as CS$_W$ SENSE, CS$_W$ SENSE with JS, and CS$_{W+TV}$ SENSE with JS; corresponding, respectively to (2), (6), and (10). As a test object, we used the analytical phantom introduced in [12] of size of 512×512, since it has many realistic anatomical aspects and can be defined with high resolution. The rectangular FOV is 25.6×25.6 cm. The sensitivity maps have been simulated with the Biot-Savart law [12], based on $C = 4$, a coil radius of 7 cm, and a distance from the coil centers to the center of the rectangular FOV of 17 cm.

TABLE I

COMPARISON OF RECONSTRUCTION ACCURACY WITH DIFFERENT CS SENSE PMRI RECONSTRUCTION AND SAMPLING METHODS

A. SER_{dB} of 512×512 Reconstructed Images			
	CS_{W} SENSE	CS_{W} SENSE with JS	$\text{CS}_{\text{W+TV}}$ SENSE with JS
(a)	16.7577	18.5484	20.3424
(b)	18.1184	20.1148	21.2058

B. $RMSE(\times 10^{-2})$ of 512×512 Reconstructed Images			
	CS_{W} SENSE	CS_{W} SENSE using JS	$\text{CS}_{\text{W+TV}}$ SENSE using JS
(a)	3.4489	2.7705	2.2976
(b)	2.9579	2.3267	2.0836

*Sampling methods (sampling percentage ≈ 10 %): (a) radial lines and (b) multi-level random sampling

For the radial line sampling method, the k-space data is sampled along 47 radial lines, uniformly-spaced in angle, corresponding to ≈ 10.0 % of the full k-space samples. For multi-level sampling, $n = 100$, $m = 0.01$, $a = 1$, and $b = 3.8822$ are used, which also leads to ≈ 10.0 % of full k-space samples. An additive noise is not considered. For the initial guess, $\mathbf{x}^{(0)} = sos(\mathit{ifft}_{2,\mathbf{C}}(\mathbf{y}))$ was obtained, where $sos(\cdot)$ denotes sum-of-squares reconstruction and $\mathit{ifft}_{2,\mathbf{C}}(\cdot)$ denotes ifft_2 for each coil. All the parameters (i.e., $\alpha, \beta, \gamma, \nu$) are selected as 1, where γ is an additional parameter to consider the TV norm in (10). The DDT filter size is 4. The stopping criterion is defined as $tol(k) = \|\mathbf{F}_{\mathbf{\Omega}}\mathbf{S}\mathbf{x}^{(k)} - \mathbf{y}\|_2^2 / \|\mathbf{y}\|_2^2$. Error minimization is evaluated with the following two measurements: $RMSE_{\log}(k) = \log_{10}\left(RMSE(\mathbf{x}^{(k)}, \mathbf{x}^{true})\right)$ and $SER_{\text{dB}}(k) = 20\log_{10}\left(\|\mathbf{x}^{true} - \mathbf{x}^{(k)}\|_2 / \|\mathbf{x}^{true}\|_2\right)$, where SER stands for signal to error ratio.

A. Reconstruction Accuracy

For both radial line and multi-level random sampling schemes, the proposed CS SENSE pMRI reconstruction promoting JS across channels shows higher reconstruction accuracy than the conventional model. Theoretically, the MC barrier in CS performance can be resolved with the multi-level sampling scheme. The radial line sampling is chosen as a practical nonuniform sampling scheme, however, it degrades the accuracy, because it takes fewer samples at low frequency than multi-level sampling. If we promote JS in both of the Wavelet and TV sparsifying domains, we can see significant SER improvement, especially for radial sampling lines, i.e. $\text{CS}_{\text{W+TV}}$ SENSE with JS can reduce the gap between the theory and practice. These assertions are supported by Fig. 2 and Table I.

B. Error Minimization Behavior

Fig. 3 shows the converging behavior of the algorithms for the convex minimization problems (2), (6), and (10). Theoretically speaking, SB is free from tricky regularization parameter selection for a constrained optimization problem: the parameter is important for convergence rate, but exhibits no effect on the solution by varying observation so called "adding back the noise" process (e.g., (4) and (8)). Even with the default setting of unity and without sophisticated control of the parameters, the algorithms show decent convergence rates.

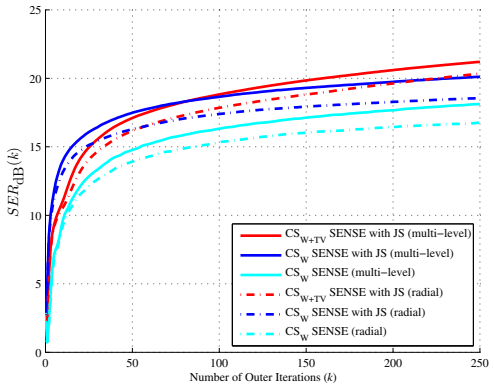

Fig. 3. Comparison of SER maximization behavior with different CS SENSE pMRI reconstruction and sampling schemes ($C = 4$, sampling percentage ≈ 10 %)

IV. CONCLUSIONS

The promotion of JS to CS SENSE pMRI reconstruction not only improves the reconstruction accuracy, but also leads to an efficient sparse recovery in Wavelet and TV domains. The radial line sampling is chosen as practical nonuniform sampling scheme to overcome the MC barrier, but limits the theoretical CS performance. This gap can be diminished by $\text{CS}_{\text{W+TV}}$ SENSE with JS. The proposed and conventional models were efficiently solved based on SB and VS.

REFERENCES

[1] B. Adcock and A. C. Hansen, "Generalized sampling and infinite-dimensional compressed sensing," DAMTP Tech. Rep. NA2011/12, University of Cambridge, Available: http://www.math.purdue.edu/~adcock/Papers/BAACHGSCS.pdf, May 2013.

[2] E. J. Candes and Y. Plan, "A probabilistic and RIPless theory of compressed sensing," *IEEE Trans. Inform. Theory*, vol. 57, no. 11, pp. 7235 – 7254, Nov. 2011.

[3] B. Adcock, A. C. Hansen, C. Poon, and B. Roman, "Breaking the coherence barrier: a new theory for compressed sensing," *ArXiv preprint cs.IT/1302.0561v3*, Feb. 2014.

[4] K. P. Pruessmann, M. Weiger, M. B. Scheidegger, and P. Boesiger, "SENSE: sensitivity encoding for fast MRI," *Magn. Reson. in Med.*, vol. 42, no. 5, pp. 952 – 962, Jul. 1999.

[5] M. F. Duarte and Y. C. Eldar, "Structured compressed sensing: From theory to applications," *IEEE Trans. Sig. Process.*, vol. 59, no. 9, pp. 4053 – 4085, Sep. 2011.

[6] P. Boufounos, G. Kutyniok, and H. Rauhut, "Sparse recovery from combined fusion frame measurements," *IEEE Trans. Inform. Theory*, vol. 57, no. 6, pp. 3864 – 3876, Jun. 2011.

[7] M. Murphy, M. Alley, J. Demmel, K. Keutzer, S. Vasanawala, and M. Lustig, "Fast l_1-SPIRiT compressed sensing parallel imaging MRI: scalable parallel implementation and clinically feasible runtime," *IEEE Trans. Med. Imag.*, vol. 31, no. 6, pp. 1250 – 1262, Jun. 2012.

[8] T. Goldstein and S. Osher, "The split Bregman method for L1-regularized problems," *SIAM Journal on Imag. Sciences*, vol. 2, no. 2, pp. 323 – 343, Apr. 2009.

[9] S. Ramani and J. A. Fessler, "A splitting-based iterative algorithm for accelerated statistical X-ray CT reconstruction," *IEEE Trans. Med. Imag.*, vol. 31, no. 3, pp. 677 – 688, Mar. 2012.

[10] H. She, R. R. Chen, D. Liang, E. V. DiBella, and L. Ying, "Sparse BLIP: BLind Iterative Parallel imaging reconstruction using compressed sensing," *Magn. Reson. in Med.*, vol. 71, no. 2, pp. 645 – 660, Feb. 2014.

[11] W. Yin, S. Osher, D. Goldfarb, and J. Darbon, "Bregman iterative algorithms for l_1-minimization with applications to compressed sensing," *SIAM Journal on Imag. Sciences*, vol. 1, no. 2, pp. 143 – 168, Mar. 2008.

[12] M. Guerquin-Kern, L. Lejeune, K. P. Pruessmann, and M. Unser, "Realistic analytical phantoms for parallel Magnetic Resonance Imaging," *IEEE Trans. Med. Imag.*, vol. 31, no. 3, pp. 626 – 636, Mar. 2012.